# Slow-Wave Bandpass Filters Using Ring or Stepped-Impedance Hairpin Resonators

Lung-Hwa Hsieh, *Student Member, IEEE,* and Kai Chang, *Fellow, IEEE*

***Abstract*—This paper proposes a new class of slow-wave bandpass filters that uses a microstrip line periodically loaded with microstrip ring or stepped-impedance hairpin resonators. The new slow-wave periodic structures utilize the parallel and series resonance characteristics of the resonators to construct a bandpass filter. Unlike conventional slow-wave filters, the proposed bandpass filters are designed to produce a narrow passband at the fundamental mode of the resonators. The new filters provide lower insertion loss than that of parallel- or cross-coupled ring and stepped-impedance hairpin bandpass filters. The calculated frequency responses of the filters agree well with experiments.**

***Index Terms*—Bandpass filter, hairpin resonator, ring resonator, slow-wave periodic structure.**

## I. Introduction

MICROSTRIP RING and stepped-impedance hairpin resonators have many attractive features and can be used in satellites, mobile phones, and other wireless communication systems. The main advantages of the resonators are their compact size, easy fabrication, narrow bandwidth, and low radiation loss. Therefore, the resonators are widely used in the design of filters, oscillators, and mixers [1, Chs. 2 and 7], [2, Ch. 4].

Some of the bandpass filters that use the ring resonator utilize the dual-mode characteristic to achieve a sharp cutoff frequency response [3]. However, the filters use perturbation notches or stubs that make their frequency response sensitive to fabrication uncertainties [3]. In addition, bandpass filters that use parallel- or cross-coupling ring resonators to produce Chebyshev- or elliptic-function characteristics [4], [5] suffer from high insertion loss. Recently, the ring resonator filters using high-temperature superconductor (HTS) and micromachined circuit technologies have demonstrated low insertion loss and a sharp cutoff frequency response, but at the expense of high fabrication costs [6].

The hairpin resonator was first introduced to reduce the size of the conventional parallel-coupled half-wavelength resonator with subsequent improvements made to reduce its size [2, Ch. 4], [7]. Beyond the advantage of the compact size, the spurious frequencies of the stepped-impedance hairpin resonator are shifted from the integer multiples of the fundamental resonant frequency due to the effect of the capacitance-load coupled lines. Also, compact size bandpass filters using stepped-impedance hairpin resonators with parallel- or cross-coupling structures have shown high insertion loss [8], [9].

An interesting slow-wave bandpass filter has been reported [10] that uses capactively loaded parallel- and cross-coupled open-loop ring resonators. This filter also shows high insertion loss.

In this paper, slow-wave bandpass filters using a microstrip line periodically loaded by ring or stepped-impedance hairpin resonators are introduced. By using the parallel and series resonance characteristics of the resonators, the slow-wave periodic structures perform as a bandpass filter. The new slow-wave bandpass filters, designed at fundamental resonant frequency of the resonators, also are different from conventional slow-wave filters, which utilize higher order modes to build up a bandpass filter with a wide passband [11] or to provide lowpass or bandstop features [12], [13]. In comparison with bandpass filters that use parallel- and cross-coupled resonators with coupling gaps between the resonators, these new slow-wave bandpass filters show lower insertion loss at similar resonant frequencies [4], [5], [8], and [9]. This is an important finding since the new filter structure uses more conductor than the parallel- and cross-coupled structures. This implies that the new filter topology significantly reduces the insertion loss caused in parallel- and cross-coupled bandpass structures by eliminating coupling gaps between resonators. The performance of the new slow-wave filters is evaluated by experiment and calculation with good agreement.

## II. Analysis of the Slow-Wave Periodic Structure

Fig. 1(a) illustrates a conventional slow-wave periodic structure. The transmission line is periodically loaded with identical open stub elements. Each unit element includes a length of $d$ transmission line with a length of $l$ open stub, where $Z_{in1}$ is the input impedance looking into the open stub. The conventional slow-wave periodic structure usually works as a low-pass or stopband filter [12], [13]. Also, using higher order modes, the conventional slow-wave periodic structure can act as a wide band bandpass filter, by constructing two consecutive stopbands close to the passband [11]. Considering the slow-wave periodic structure in Fig. 1(b), a loading impedance $Z_L$ is connected at the end of the open stub. The input impedance $Z_{in2}$ is given by

$$Z_{in2} = Z_o \frac{Z_L + jZ_o \tan(\beta l)}{Z_o + jZ_L \tan(\beta l)} \qquad \text{for lossless line} \quad (1)$$

where $Z_o$ and $\beta$ are the characteristic impedance and phase constant of the open stub, respectively. If $Z_L = \infty$ or $0$ with a very small value of $\tan(\beta l)$, the input impedance $Z_{in2} \to \infty$ or $0$, respectively. Under these cases, the slow-wave periodic structure

Manuscript received July 5, 2001.

The authors are with the Department of Electrical Engineering, Texas A&M University, College Station, TX 77843-3128 USA (e-mail: welber@ee.tamu.edu; chang@ee.tamu.edu).

Publisher Item Identifier 10.1109/TMTT.2002.800439.

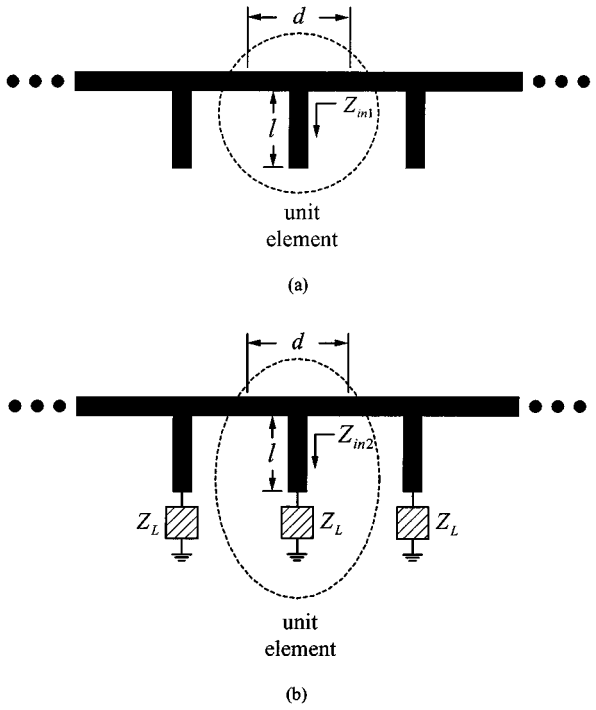


Fig. 1. Slow-wave periodic structure. (a) Conventional type. (b) With loading $Z_L$ at open end.

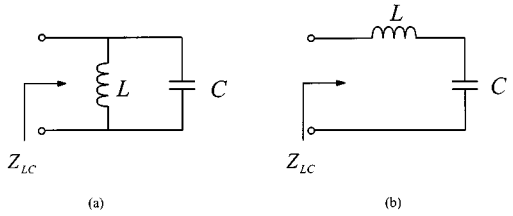


Fig. 2. Lossless (a) parallel and (b) series resonant circuits.

loaded by $Z_{in2}$ in Fig. 1(b) provides passband ($Z_{in2} \rightarrow \infty$) and stopband ($Z_{in2} \rightarrow 0$) characteristics. For example, the conventional capacitance-load Kuroda-identity periodic structure is the case of $Z_L = \infty$ with $l = \lambda_g/8$ [14, Ch. 8].

Fig. 2 shows lossless parallel and series resonant circuits. At resonance, the input impedance $Z_{LC}$ of the parallel and series resonant circuits is $\infty$ and 0, respectively. The input impedance $Z_{LC}$ of the resonant circuits can act as the loading impedance $Z_L$ in Fig. 1(a) for the passband and stopband characteristics of a slow-wave periodic structure. In practice, for the high $Q$ ring and hairpin resonators, the input impedance of the resonators shows very large and small values at parallel and series resonant frequencies, respectively. Thus, a slow-wave periodic structure loaded by ring or hairpin resonators with two series resonant frequencies close to a parallel resonant frequency [1, Chs. 2 and 7], [2, Ch. 4] can be designed for a bandpass filter at fundamental mode.

The key point behind this new slow-wave filter topology is that both the series and the parallel resonances of the loading circuit are used to achieve bandpass characteristics. The approach can, in fact, be interpreted as using the stopbands of two series resonances in conjunction with the passband of a parallel resonance to achieve a bandpass frequency response. It is noted, however, that in some cases, undesired passbands below and above the main passband may require a high-pass or bandpass section to be used in conjunction with this approach.

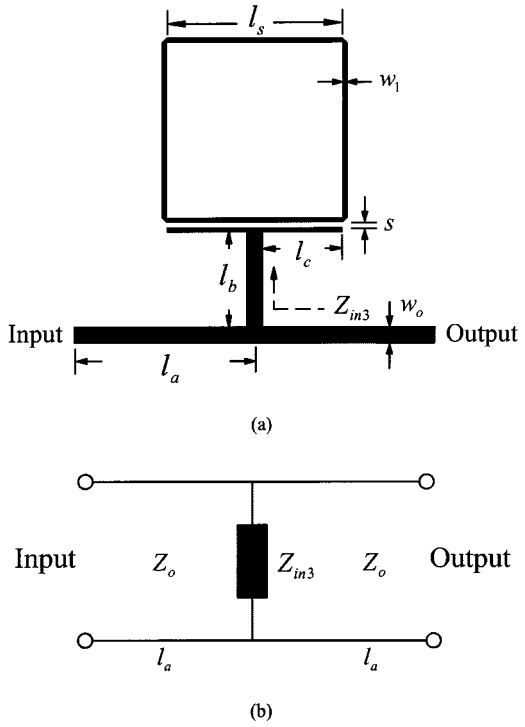


Fig. 3. Slow-wave bandpass filter using one ring resonator with one coupling gap. (a) Layout. (b) Simplified equivalent circuit.

## III. Slow-Wave Bandpass Filters Using Square Ring Resonators

Fig. 3 shows a transmission line loaded by a square ring resonator with a line-to-ring coupling structure and its simple equivalent circuit, where $Z_{in3}$ is the input impedance looking into the transmission line $l_b$ toward the ring resonator with the line-to-ring coupling. As seen in Fig. 4(a), the coupling structure includes the coupling line, one side of the square ring resonator and a coupling gap. This coupling structure can be treated as symmetrical coupled lines [15]. The coupling gap between the symmetrical coupled lines is modeled as a capacitive L-network as shown in Fig. 4(b) [16]. $C_g$ is the gap capacitance per unit length, and $C_p$ is the capacitance per unit length between the strip and the ground plane. These capacitances, $C_g$ and $C_p$, can be found from the even- and odd-mode capacitances of symmetrical coupled lines [17, Ch. 3]. Fig. 4(c) shows the equivalent circuit of the capacitive L-network, where the input impedance of the ring resonator $Z_r$ can be obtained from [16]. The input impedance $Z_{r1}$ looks into the line-to-ring coupling structure toward the ring resonator. The input impedance $Z_{in3}$ is

$$Z_{in3} = Z_o \frac{Z_{r1} + jZ_o \tan(\beta l_b)}{Z_o + jZ_{r1} \tan(\beta l_b)} \tag{2}$$

where $Z_{r1} = (Z_r + Z_g) \| Z_p$, $Z_g = 1/j\omega C_g \Delta l$, $Z_p = 1/j\omega C_p \Delta l$, and $\omega$ is the angular frequency. The

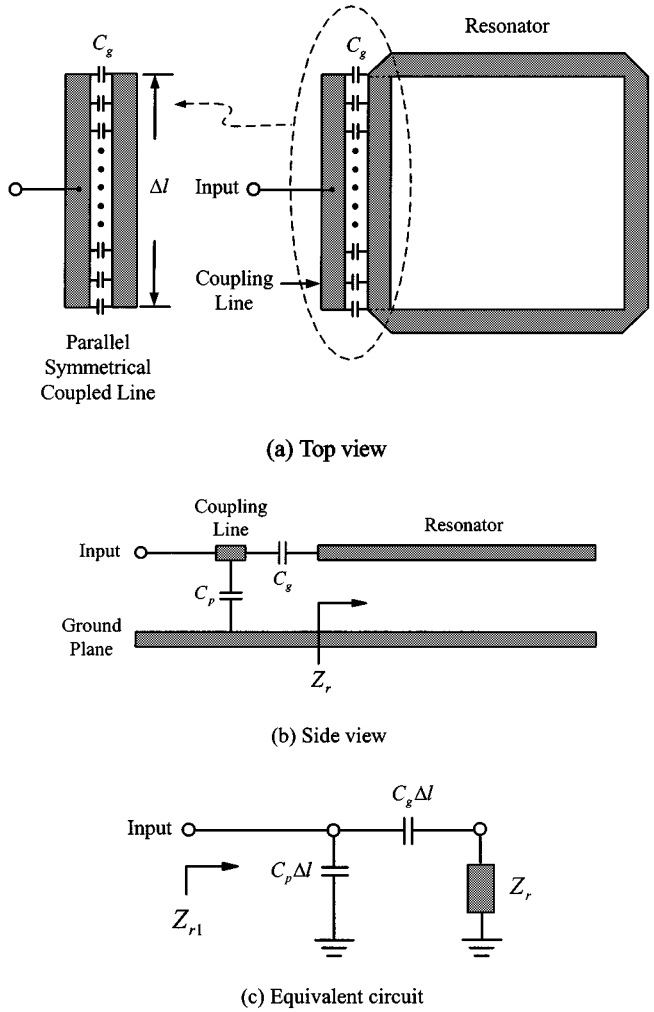


Fig. 4. Line-to-ring coupling structure. (a) Top view. (b) Side view. (c) Equivalent circuit.

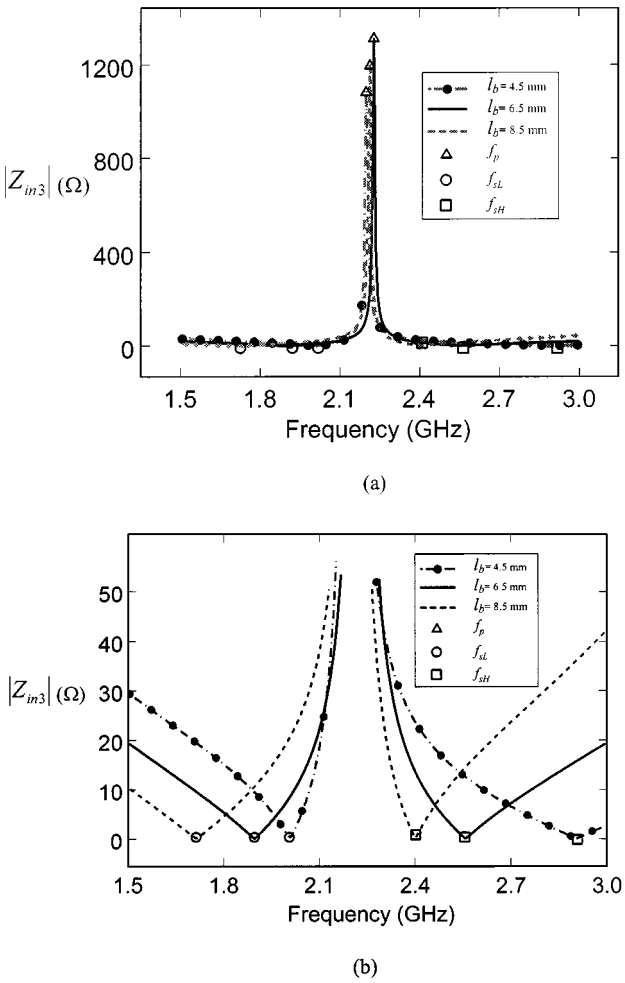


Fig. 5. Variation in input impedance $|Z_{in3}|$ for different lengths of $l_b$ showing: (a) parallel and series resonances and (b) an expanded view for the series resonances.

parallel $(f_p)$ and series $(f_s)$ resonances of the ring resonator can be obtained by setting

$$|Y_{in3}| = |1/Z_{in3}| \sim 0 \text{ and } |Z_{in3}| \sim 0. \tag{3}$$

The frequency response of the ring circuit can be calculated using the equivalent circuit in Fig. 3(b). The $ABCD$ matrix of the ring circuit is

$$\begin{aligned}\begin{bmatrix} A & B \\ C & D \end{bmatrix} &= \begin{bmatrix} \cos(\beta l_a) & jZ_o\sin(\beta l_a) \\ jY_o\sin(\beta l_a) & \cos(\beta l_a) \end{bmatrix} \begin{bmatrix} 1 & 0 \\ Y_{in3} & 1 \end{bmatrix} \\ &\quad \cdot \begin{bmatrix} \cos(\beta l_a) & jZ_o\sin(\beta l_a) \\ jY_o\sin(\beta l_a) & \cos(\beta l_a) \end{bmatrix} \\ &= \begin{bmatrix} 1-2\sin^2(\beta l_a)+jZ_oY_{in3}\sin(\beta l_a)\cos(\beta l_a) \\ Y_{in3}\cos^2(\beta l_a)+j2Y_o\sin(\beta l_a)\cos(\beta l_a) \\ -Z_o^2Y_{in3}\sin^2(\beta l_a)+j2Z_o\sin(\beta l_a)\cos(\beta l_a) \\ 1-2\sin^2(\beta l_a)+jZ_oY_{in3}\sin(\beta l_a)\cos(\beta l_a) \end{bmatrix}\end{aligned} \tag{4}$$

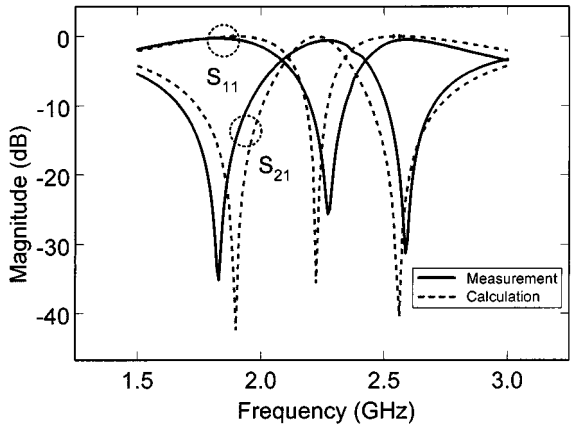


Fig. 6. Measured and calculated frequency response for the slow-wave bandpass filter using one square ring resonator.

where $Y_o = 1/Z_o$. Using $Y_{in3}(f_p)$ and $Z_{in3}(f_s)$, the passband and stopband of the ring circuit can be obtained by calculating $S_{11}$ and $S_{21}$ from the $ABCD$ matrix in (4).

The ring circuit was designed at the center frequency of 2.4 GHz and fabricated on a RT/Duroid 6010.5 substrate with a thickness $h = 50$ mil and a relative dielectric constant

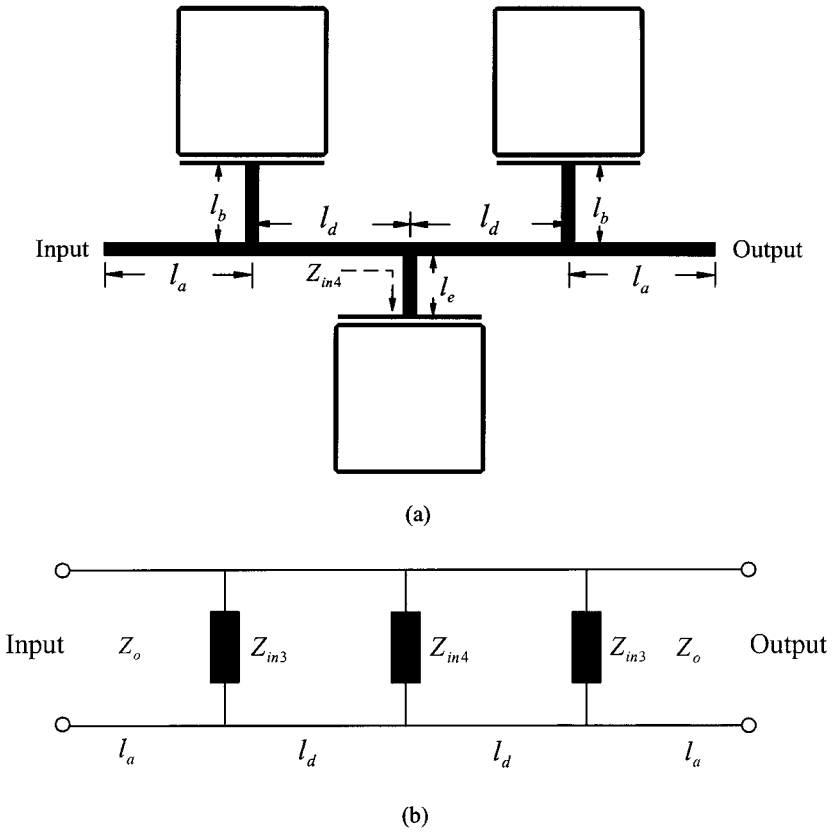


Fig. 7. Slow-wave bandpass filter using three ring resonators. (a) Layout. (b) Simplified equivalent circuit.

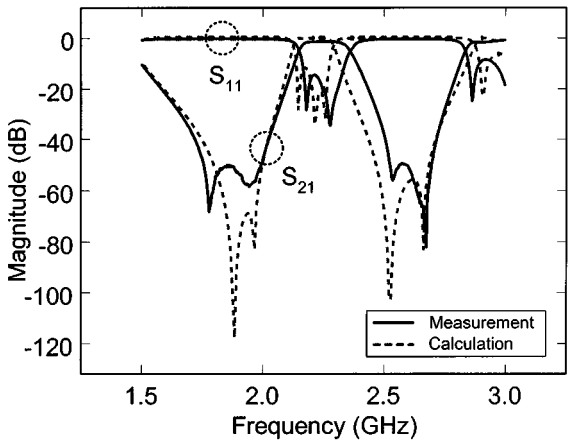


Fig. 8. Measured and calculated frequency response for the slow-wave bandpass filter using three square ring resonators.

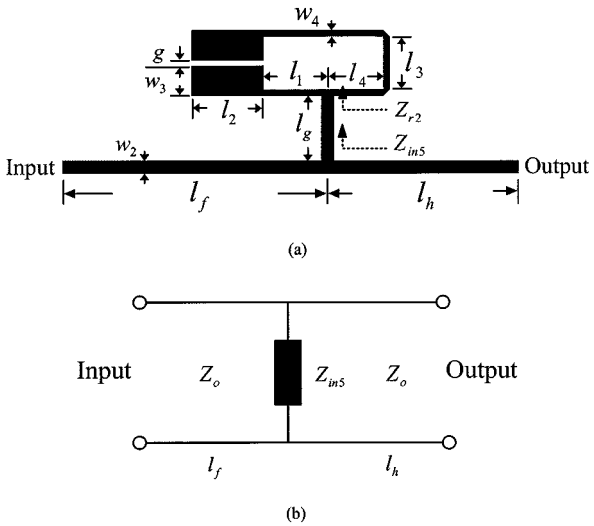


Fig. 9. Slow-wave bandpass filter using one stepped-impedance hairpin resonator. (a) Layout. (b) Simplified equivalent circuit.

$\varepsilon_r = 10.5$. The dimensions of the filter are $l_s = 12.07$ mm, $s = 0.2$ mm, $l_a = 12.376$ mm, $l_b = 6.5$ mm, $w_o = 1.158$ mm, $w_1 = 0.3$ mm. These parameter values are synthesized from the design equations using numerical optimization to construct a bandpass filter with attenuation poles centered at $\pm 330$ MHz about the parallel resonant frequency. Fig. 5(a) shows the calculated input impedance $Z_{in3}$ with parallel and two series resonances of the ring resonator at different lengths of $l_b$. The parallel $(f_p)$, lower $(f_{sL})$ and higher $(f_{sH})$ series resonances corresponding to the passband and stopband of the ring circuit in Fig. 3 are denoted by $\triangle$, $\bigcirc$, and $\square$, respectively. By adjusting the length of $l_b$ properly, the parallel resonance can be centered between two series resonances. Also, Fig. 5(b) shows an extended view for series resonances. The measured and calculated frequency response of the ring circuit is illustrated in Fig. 6. The filter has a fractional 3-dB bandwidth of 15.5%. The insertion and return losses are 0.53 and 25.7 dB at 2.3 GHz, respectively. Two attenuation poles are at 1.83 and 2.59 GHz with attenuation level of 35.2 and 31.3 dB, respectively. The measured unloaded $Q$ of the closed-loop ring resonator is 122.

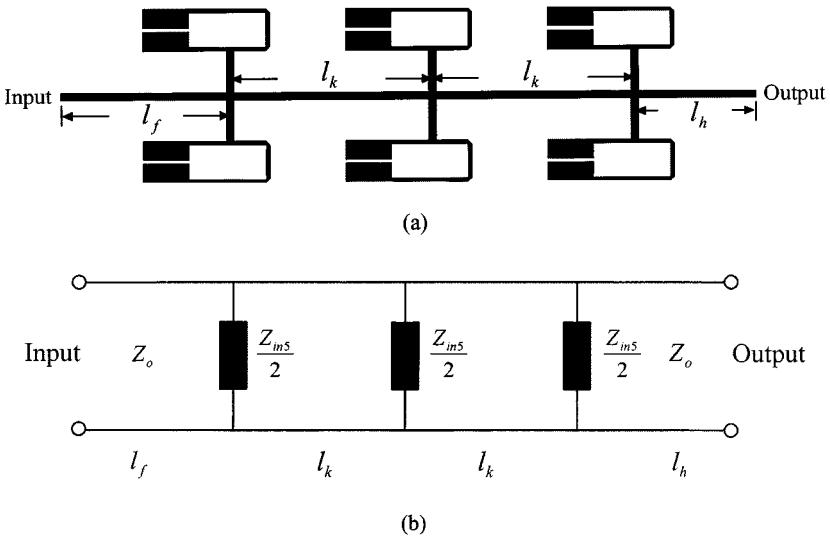


Fig. 10. Slow-wave bandpass filter using six stepped-impedance hairpin resonators. (a) Layout. (b) Simplified equivalent circuit.

To improve the passband and rejection, a slow-wave bandpass filter using three ring resonators has also been built. As seen in Fig. 7, the transmission line is loaded periodically by three ring resonators, where $Z_{in4}$ is the input impedance looking into $l_e$ toward the ring. The filter uses the same dimensions as the filter with a single ring resonator in Fig. 3, but with the transmission lengths $l_d = 15.686$ mm and $l_e = 5.5$ mm, which are optimized by the calculation equations to obtain wider stopbands than the filter in Fig. 3. The frequency response of the filter can be obtained from $ABCD$ matrix of the equivalent circuit in Fig. 7(b). Fig. 8 illustrates the measured and calculated results. The filter with an elliptic-function characteristic has a 3-dB fractional bandwidth of 8.5% and a passband from 2.16 to 2.34 GHz with return loss better than 10 dB. The maximum insertion loss in the passband is 1.45 dB with a ripple of $\pm$0.09 dB. In addition, the two stop bands exhibit a rejection level larger than 50 dB within 1.76–2 GHz and 2.52–2.7 GHz. Observing the frequency response of the filters in Figs. 6 and 8, the differences between the calculated and measured results are due to the use of a lossless calculation model.

## IV. Slow-Wave Bandpass Filters Using Stepped-Impedance Hairpin Resonators

The hairpin has parallel and series resonance characteristics and can also be used as the loading impedance $Z_L$ in the slow-wave periodic structure of Fig. 1(b) to construct a bandpass response. Fig. 9 shows the filter using one stepped-impedance hairpin resonator and its simple equivalent circuit, where $Z_{in5}$ is the input impedance looking into $l_g$ toward the resonator. $Z_{r2}$, the input impedance of the stepped-impedance hairpin resonator, can be obtained from [2, Ch. 4]. Similar to the ring circuit in Fig. 3, the frequency response of the hairpin circuit can also be obtained from the $ABCD$ matrix of the equivalent circuit in Fig. 9(b). The filter was designed at the center frequency of 2 GHz and fabricated on a RT/Duroid 6010.2 substrate with thickness $h = 25$ mil and a relative dielectric constant $\varepsilon_r = 10.2$. The parameters of the filter are shown as

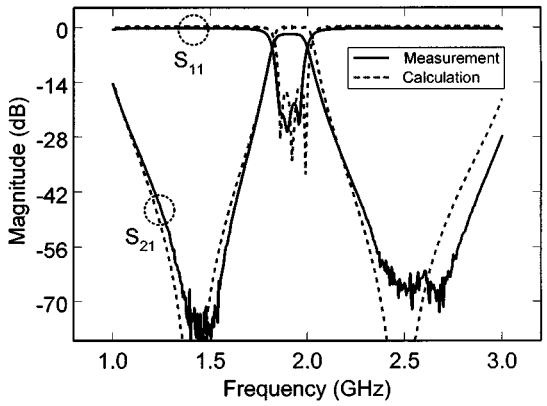


Fig. 11. Measured and calculated frequency response for the slow-wave bandpass filter using six stepped-impedance hairpin resonators.

follows: $l_g = 3$ mm, $l_1 = 3$ mm, $l_2 = 3.35$ mm, $l_3 = 2.5$ mm, $l_4 = 2.596$ mm, $w_2 = 0.591$ mm, $w_3 = 1.425$ mm, $w_4 = 0.3$ mm, $g = 0.25$ mm, $l_f = 12.345$ mm, and $l_h = 8.9$ mm. These parameter values are synthesized from the design equations, similar to (4), using numerical optimization to build a bandpass filter with attenuation poles centered at $\pm$530 MHz about the parallel resonant frequency. Calculated and measured results similar to Figs. 5 and 6 have been obtained. Also, by adjusting the length of $l_g$ properly, the two series resonances can be centered about the parallel resonance when $l_g = 3$ mm.

Fig. 10 shows the transmission line loaded periodically by six stepped-impedance hairpin resonators. The filter uses the same dimensions as the filter using a single hairpin resonator in Fig. 9, but with the transmission length $l_k = 14.755$ mm, which is optimized by the calculation equations for maximum rejection. Fig. 11 illustrates the measured and calculated results. The filter with a Chebyshev characteristic has a 3-dB fractional bandwidth of 8.55%. A passband is from 1.84 to 1.98 GHz with a return loss better than 10 dB. The maximum insertion loss in the passband is 1.82 dB with a ripple of $\pm$0.06 dB. In addition, two stopbands exhibit a rejection level greater than 60 dB within

1.32–1.57 and 2.38–2.76 GHz. The measured unloaded $Q$ of the stepped-impedance hairpin resonator is 146. Due to the use of the lossless model for calculation, these calculated responses show small differences from measured results.

## V. Conclusions

Novel slow-wave bandpass filters using a microstrip line periodically loaded with ring or stepped-impedance hairpin resonators are proposed. By using the parallel and series resonance characteristics of the resonators, the new slow-wave periodic structures behave as bandpass filters. The new filters with a narrow passband designed at the fundamental mode of the resonators are different from the conventional slow-wave filters. Furthermore, the new filters have lower insertion loss than those of filters using parallel- or cross-coupled ring and stepped-impedance hairpin resonators. The filters have been investigated by experiment and calculation with good agreement.

## Acknowledgment

The authors would like to thank C. Wang, Texas A&M University, College Station, for his technical assistance and C. Rodenbeck, Texas A&M University, for his helpful discussions.

## References

[1] K. Chang, *Microwave Ring Circuits and Antennas*. New York: Wiley, 1996.
[2] M. Makimoto and S. Yamashita, *Microwave Resonators and Filters for Wireless Communication Theory, Design and Application*. Berlin, Germany: Springer-Verlag, 2001.
[3] L. Zhu and K. Wu, "A joint field/circuit model of line-to-ring coupling structures and its application to the design of microstrip dual-mode filters and ring resonator circuits," *IEEE Trans. Microwave Theory Tech.*, vol. 47, pp. 1938–1948, Oct. 1999.
[4] C. C. Yu and K. Chang, "Novel compact elliptic-function narrow-band bandpass filters using microstrip open-loop resonators with coupled and crossing lines," *IEEE Trans. Microwave Theory Tech.*, vol. 46, pp. 952–958, July 1998.
[5] J. S. Hong and M. J. Lancaster, "Couplings of microstrip square open-loop resonators for cross-coupled planar microwave filters," *IEEE Trans. Microwave Theory Tech.*, vol. 44, pp. 2099–2109, Nov. 1996.
[6] J. S. Hong, M. J. Lancaster, D. Jedamzik, R. B. Greed, and J. C. Mage, "On the performance of HTS microstrip quasielliptic function filters for mobile communications application," *IEEE Trans. Microwave Theory Tech.*, vol. 48, pp. 1240–1246, July 2000.
[7] J. S. Wong, "Microstrip tapped-line filter design," *IEEE Trans. Microwave Theory Tech.*, vol. MTT-27, pp. 44–50, Jan. 1979.
[8] M. Sagawa, K. Takahashi, and M. Makimoto, "Miniaturized hairpin resonator filters and their application to receiver front-end MIC's," *IEEE Trans. Microwave Theory Tech.*, vol. 37, pp. 1991–1997, Dec. 1989.
[9] J. T. Kuo, M. J. Maa, and P. H. Lu, "A microstrip elliptic function filter with compact miniaturized hairpin resonators," *IEEE Microwave Guided Wave Lett.*, vol. 10, pp. 94–95, Mar. 2000.
[10] J. S. Hong and M. J. Lancaster, "Theory and experiment of novel microstrip slow-wave open-loop resonator filters," *IEEE Trans. Microwave Theory Tech.*, vol. 45, pp. 2358–2365, Dec. 1997.
[11] J. P. Hsu, T. Anada, H. Tsubaki, Y. Migita, and K. Nagashima, "Synthesis of planar microwave band-pass filter based on foster-type network and normal mode expansion method," in *IEEE MTT-S Int. Microwave Symp. Dig.*, 1992, pp. 1199–1202.
[12] F. R. Yang, K. P. Ma, Y. Qian, and T. Itoh, "A uniplanar compact photonic-bandgap (UC-PBG) structure and its applications for microwave circuits," *IEEE Trans. Microwave Theory Tech.*, vol. 47, pp. 1509–1514, Aug. 1999.
[13] H. C. Bell, "Narrow bandstop filters," *IEEE Trans. Microwave Theory Tech.*, vol. 39, pp. 2188–2191, Dec. 1991.
[14] D. M. Pozar, *Microwave Engineering*, 2nd ed. New York: Wiley, 1998.
[15] G. Kumar and K. C. Gupta, "Broad-band microstrip antennas using additional resonators gap-coupled to the radiating edges," *IEEE Trans. Antennas Propagat.*, vol. AP-32, pp. 1375–1379, Dec. 1984.
[16] C. C. Yu and K. Chang, "Transmission-line analysis of a capacitively coupled microstrip-ring resonator," *IEEE Trans. Microwave Theory Tech.*, vol. 45, pp. 2018–2024, Nov. 1997.
[17] R. Mongia, I. Bahl, and P. Bhartia, *RF and Microwave Coupled-Line Circuits*. Norwood, MA: Artech House, 1999.

**Lung-Hwa Hsieh** (S'01) was born in Panchiao, Taiwan, R.O.C., in 1969. He received the B.S. degree in electrical engineering from Chung Yuan Christian University, Chungli, Taiwan, R.O.C., in 1991, the M.S. degree in electrical engineering from the National Taiwan University of Science and Technology, Taipei, Taiwan, R.O.C., in 1993, and is currently working toward the Ph.D. degree in electrical engineering at Texas A&M University, College Station.

From 1995 to 1998, he was a Senior Design Engineer with General Instrument, Taipei, Taiwan, R.O.C., where he was involved in RF video and audio circuit design. Since 2000, he has been a Research Assistant in the Department of Electrical Engineering, Texas A&M University. His research interests include microwave integrated circuits and devices.

**Kai Chang** (S'75–M'76–SM'85–F'91) received the B.S.E.E. degree from the National Taiwan University, Taipei, Taiwan, R.O.C., in 1970, the M.S. degree from the State University of New York at Stony Brook, in 1972, and Ph.D. degree from The University of Michigan at Ann Arbor, in 1976.

From 1972 to 1976, he worked for the Microwave Solid-State Circuits Group, Cooley Electronics Laboratory, The University of Michigan at Ann Abor, as a Research Assistant. From 1976 to 1978, he was with Shared Applications Inc., Ann Arbor, MI, where he was involved with computer simulation of microwave circuits and microwave tubes. From 1978 to 1981, he was with the Electron Dynamics Division, Hughes Aircraft Company, Torrance, CA, where he was involved in the research and development of millimeter-wave solid-state devices and circuits, power combiners, oscillators, and transmitters. From 1981 to 1985, he was with TRW Electronics and Defense, Redondo Beach, CA, where he was a Section Head, involved with the development of state-of-the-art millimeter-wave integrated circuits and subsystems including mixers, VCOs, transmitters, amplifiers, modulators, upconverters, switches, multipliers, receivers, and transceivers. In August 1985, he joined the Department of Electrical Engineering, Texas A&M University, College Station, as an Associate Professor, and was promoted to a Professor in 1988. In January 1990, he was appointed E-Systems Endowed Professor of Electrical Engineering. His current interests are in microwave and millimeter-wave devices and circuits, microwave integrated circuits, integrated antennas, wide-band and active antennas, phased arrays, microwave power transmission, and microwave optical interactions.

Dr. Chang has authored or coauthored *Microwave Solid-State Circuits and Applications* (New York: Wiley, 1994), *Microwave Ring Circuits and Antennas* (New York: Wiley, 1996), *Integrated Active Antennas and Spatial Power Combining* (New York: Wiley, 1996), *RF and Microwave Wireless Systems* (New York: Wiley, 2000), and *RF and Microwave Circuit and Component Design for Wireless Systems* (New York, Wiley, 2002). He also served as the editor of the four-volume *Handbook of Microwave and Optical Components*(New York: Wiley, 1989 and 1990). He is the editor of *Microwave and Optical Technology Letters* and the Wiley Book Series in *Microwave and Optical Engineering*. He has authored or coauthored over 350 technical papers and several book chapters in the areas of microwave and millimeter-wave devices, circuits, and antennas.

Dr. Chang received the Special Achievement Award from TRW in 1984, the Halliburton Professor Award in 1988, the Distinguished Teaching Award in 1989, the Distinguished Research Award in 1992, and the TEES Fellow Award in 1996 from Texas A&M University.